JOURNAL OF GEOPHYSICAL RESEARCH: OCEANS, VOL. 119, 266–275, doi:10.1002/2013JC009327, 2014

Decadal sea-level variability along the coast of Japan in response to ocean circulation changes

Yoshi N. Sasaki,[1] Shoshiro Minobe,[1] and Yuji Miura[2]

Received 5 August 2013; revised 19 December 2013; accepted 20 December 2013; published 16 January 2014.

[1] Decadal sea-level variability along the coast of Japan and its relation to large-scale ocean circulation changes from 1993 to 2010 was investigated using tide-gauge and satellite-derived sea-level data. A singular value decomposition (SVD) analysis is performed between coastal sea levels of Japan and sea levels in the western North Pacific. The first SVD mode reveals that the northward shifts of the Kuroshio Extension (KE) jet and the Kuroshio southeast of Japan accompany the coastal sea-level rise in the early 2000s and 2010, and their southward shifts accompany the coastal sea-level fall in the late 1990s and the late 2000s. The shifts of the KE jet are induced by westward propagating Rossby wave from the eastern North Pacific, which is concentrated along the KE jet axis as jet-trapped Rossby waves. The resulting sea-level changes along the coast of Japan show a strong spatial contrast. The sea-level fluctuation is quite large along the southeastern coast of Japan that is under the direct influence of the jet-trapped Rossby waves, and also large in the western coast of Japan, probably due to coastal waves that are excited by the incoming Rossby waves, but is small north of the KE jet latitude. Hence, the nature of the wave trapped by the KE jet produces an "active zone" and a "shadow zone" of coastal sea-level variability of Japan. Our results indicate that the correct representation of western boundary currents is necessary for reliable prediction of future coastal sea-level changes.

Citation: Sasaki, Y. N., S. Minobe, and Y. Miura (2014), Decadal sea-level variability along the coast of Japan in response to ocean circulation changes, *J. Geophys. Res. Oceans*, *119*, 266–275, doi:10.1002/2013JC009327.

1. Introduction

[2] Long-term sea-level variability, especially sea-level rise has attracted much attention because of not only its importance on coastal environment and society but also a manifestation of the global warming [e.g., *Church*, 2001; *Cazenave and Nerem*, 2004; *Merrifield et al*., 2009; *Nerem et al*., 2010; *Church et al*., 2011; *Vinogradov and Ponte*, 2011; *Sallenger et al*., 2012]. Recent studies revealed from satellite altimeter observations that the global mean sea-level rise was about $+3.1$ mm yr^{-1} during the period 1993–2003 [*Ishii et al*., 2006; *Bindoff et al*., 2007; *Suzuki and Ishii*, 2011b]. Importantly, the sea-level rise is not globally uniform. During the satellite era, sea level tended to rise significantly in the western part of the Pacific and the eastern Indian Ocean, and tended to fall in the eastern Pacific and the western Indian Ocean [e.g., *Cazenave and Nerem*, 2004; *Bindoff et al*., 2007; *Zhang and Church*, 2012]. Upper ocean circulation changes in response to surface wind forcing induce this spatial dependency of the sea-level change in the Pacific [e.g., *Qiu and Chen*, 2006; *Sasaki et al*., 2008; *Timmermann et al*., 2010; *Bromirski et al*., 2011]. However, the relation between the ocean circulation changes in the Pacific and coastal sea-level changes is not fully understood. In particular, these relations are not straightforward in the midlatitude western Pacific [e.g., *Holbrook et al*., 2011], where there are strong western boundary currents. In the case of the North Pacific, a large sea-level rise occurs in the North Pacific subtropical gyre from satellite observations [e.g., *Cazenave and Nerem*, 2004; *Bindoff et al*., 2007]. It is well known that the upper ocean changes associated with wind forcing propagate westward as a long Rossby wave [e.g., *Anderson and Killworth*, 1979; *Qiu*, 2003; *Hong et al*., 2000; *Sasaki and Schneider*, 2011a]. Recently, *Sasaki et al*. [2013] showed from satellite data that signals were propagating westward from the eastern North Pacific around 30°–40°N and becoming concentrated on the Kuroshio Extension (KE) jet axis as jet-trapped Rossby waves [*Sasaki and Schneider*, 2011a, 2011b] in the KE region in contrast to a traditional linear long Rossby wave theory [e.g., *Anderson and Killworth*, 1979; *Gill*, 1982]. One of the most likely places to be affected by these Rossby waves from the North Pacific subtropical gyre is the coast of Japan (see Figure 1a), which is one of the most densely populated areas of the world. In addition, a large sea-level rise in the North Pacific subtropical gyre has been also predicted by climate model simulations of the global warming scenario [e.g., *Meehl et al*., 2007; *Yin et al*., 2010; *Suzuki and Ishii*, 2011a].

[1]Graduate School of Science, Hokkaido University, Sapporo, Japan.
[2]Geospatial Information Authority of Japan, Tsukuba, Japan.

Corresponding author: Y. N. Sasaki, Graduate School of Science, Hokkaido University, Science 8th Bldg. 8-3-20, N10, W8, Sapporo 060-0810, Japan. (sasakiyo@mail.sci.hokudai.ac.jp)

2169-9275/14/10.1002/2013JC009327

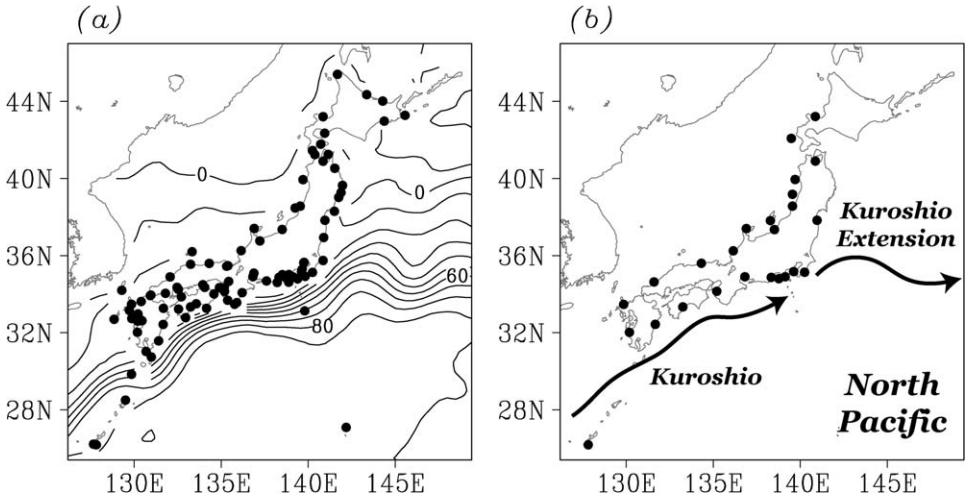

Figure 1. Tide-gauge station locations for (a) PSMSL and (b) the Geodetic Observation Center in the Geospatial Information Authority of Japan. The contour in Figure 1a denotes climatology of the mean sea surface dynamic topography [*Maximenko et al*., 2009], and the contour interval is 10 cm.

Consistently, the OECD (Organization for Economic Co-Operation and Development) report [*Nicholls et al*., 2008] selected three cities along the North Pacific coast of Japan as the top 20 cities ranked in terms of assets exposed to coastal flooding in the 2070s [see also *Nicholls and Cazenave*, 2010]. Therefore, clarification of the response of the coastal sea levels of Japan to sea-level changes of the North Pacific subtropical gyre is highly desired.

[3] Some observational and modeling studies have investigated sea-level changes along the coast of Japan on decadal and longer timescales. *Senjyu et al*. [1999] and *Senjyu* [2006] reported a bidecadal variation of coastal sea levels across all of Japan based on tide-gauge data, and *Yasuda and Sakurai* [2006] argued, using an ocean general circulation model, that this bidecadal variability was a result of westward propagation of linear long Rossby waves from the central and eastern North Pacific. Bidecadal oceanic anomalies may be forced by bidecadal atmospheric circulation anomalies, which were found to be correlated with the strength changes of Aleutian lows [*Minobe* 1999, 2000; *Minobe et al*., 2002]. *Cui et al*. [1995] showed a statistical relationship of decadal variability of coastal sea level along Japan to sea-level pressure fluctuations over the eastern North Pacific. Furthermore, the large meander path of the Kuroshio south of Japan [e.g., *Kawabe*, 1995] was shown to induce large sea-level changes along the southern coast of Japan [*Kawabe*, 1987; *Senjyu et al*., 1999]. Nevertheless, although the satellite altimeter data sets give information about ocean circulation changes, the response of the coastal sea level along Japan to ocean circulation changes has not yet been investigated using satellite data.

[4] The purpose of this paper is, therefore, to clarify sea-level variability along the coast of Japan in response to large-scale ocean circulation changes using observational data sets. In particular, we examine the spatial dependency of coastal sea-level changes around Japan and the causes of the spatial dependency. The rest of the present paper is organized as follows: observational sea-level data and the methods are reviewed in section 2. The spatial dependency of the coastal sea level of Japan and its relation to large-scale ocean circulation changes are examined in section 3. We summarize the results and discuss the importance of western boundary currents for future sea-level changes in section 4.

2. Data and Methods

2.1. Observational Data

[5] Monthly sea-level anomaly (SLA) and absolute dynamic height data were obtained from the satellite altimetry combined observations from TOPEX/Poseidon, ERS-1/2, Jason-1, and Envisat on a 1/3° × 1/3° Mercator grid from January 1993 to December 2010 from Archiving, Validation and Interpretation of Satellite Oceanographic data (AVISO) [*Ducet and Le Traon*, 2001]. The absolute dynamic height data of this data set was determined by applying the mean dynamic topography [*Rio and Hernandez*, 2004].

[6] To investigate sea-level variability along the coast of Japan, two tide-gauge data sets were employed. One was taken from the Permanent Service for Mean Sea Level (PSMSL) [*Woodworth and Player*, 2003]. We used monthly data during the period from January 1993 to December 2010, matched to the same period available from the AVISO data. The 95 stations along the coast of Japan employed in the present study are shown in Figure 1a and we do not include data from tide-gauge stations having more than 20% missing data during the period, or the Kobe II station data (34.68°N, 135.19°E), which showed a sudden sea-level rise around January 1995, probably due to the Great Hanshin Earthquake. Correction for atmospheric pressure effects was applied to the tide-gauge data using the Japanese 25 year reanalysis/Japan Meteorology Agency Climate Data Assimilation System (JRA25/JCDAS) reanalysis product with 1.25° × 1.25° spatial resolution [*Onogi et al*., 2007]. Results are robust if instead sea-level pressure of the ERA-interim reanalysis [*Dee et al*., 2011] is used. The other tide-gauge data set was obtained from the Geodetic Observation Center in the Geospatial Information Authority of Japan. The sea levels of this data set are

available only after the early 2003, but are corrected not only for atmospheric pressure effects and tidal motion but also for vertical movement of the land using Global Positioning System (GPS) measurements [*Miura and Kawamoto*, 2012]. Hence, this data set provides the necessary information to determine whether the observed sea-level changes are induced by land movements. This data set gives daily sea-level values for 25 stations (Figure 1b). We calculate a monthly mean value for all months for which data for 15 days or more were available in a month. If there are less than 15 days of data in a month, the value of that month is missing.

2.2. Methods

[7] To understand the relation between sea-level variability along the coast of Japan and in the western North Pacific, we employed singular value decomposition (SVD) analysis, which extracts maximum covariability based on a covariance matrix constructed from two variables [*Bretherton et al*., 1992]. In this study, one variable is SLAs of the altimeter data in the western North Pacific (25°–50°N, 125°–165°E), and the other variable is SLAs of the PSMSL tide-gauge data along the coast of Japan (Figure 1a). Before the analysis, the coastal sea levels are normalized by the standard deviation of each tide-gauge station to achieve similar weighting for data from each station. We will show a heterogeneous map for the coastal sea level and a homogeneous map for the large-scale SLAs, because this representation produces a linear relation between the two variables [*Czaja and Frankignoul*, 2002] and makes it possible to quantitatively compare the two variables. The statistical significance of the correlation coefficients were estimated by a Monte-Carlo test using 1000 random time series that are made by a phase randomization technique [*Kaplan and Glass*, 1995]. In this technique, surrogate time series are produced using observed spectrum and randomized phases and, thus, timescales in the original time series are preserved in the surrogate ones.

[8] Since our focus is a long-term sea-level fluctuation in addition to globally uniform sea-level rise, the global mean linear sea-level trend during the satellite era of +3.0 mm yr^{-1}, which is estimated from the satellite SLA data, is removed from all sea-level data. This is equivalent to the assumption that coastal sea-level variability along the coast of Japan is the sum of a globally uniform trend and regional-dependent variability. This method can also give us insight into regional sea-level rise. Figure 2 shows a histogram of linear sea-level trends at each station along the coast of Japan of the PSMSL data set. The mean and median values of these sea-level trends are +2.94 and +3.37 mm yr^{-1}, respectively, and are close to the global mean linear sea-level trend. Thus, our assumption is likely to be reasonable. Note that the spatial pattern of these trends is not well organized (not shown). Also, we checked the linear trend along the coast of Japan before the satellite observations. The mean and median values of the sea-level trends along the coast of Japan from 1961 to 2003 are +1.43 and +1.62 mm yr^{-1}, respectively, although the number of the stations decreases from 95 to 59. These values are comparable to the global mean sea-level trend (e.g., $+1.8 \pm 0.5$ mm yr^{-1}) [*Bindoff et al*., 2007]. Hence, our assumption seems to be true at least from 1961. In addition to removing the global mean linear trend, we subtract monthly mean climatology from each sea-level time series, and all sea-level time series are smoothed with a 9 month running mean filter to remove intraseasonal variability.

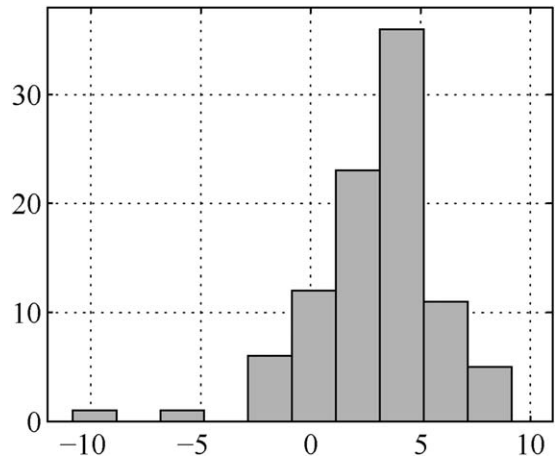

Figure 2. Histogram of the linear trend of sea level (mm yr^{-1}) based on PSMSL tide-gauge station data obtained during the period 1993–2010.

3. Results

3.1. Dominant Sea-Level Variability in the Western North Pacific

[9] To clarify the relation between sea-level changes along the coast of Japan and in the western North Pacific, we performed the SVD analysis. Figure 3 shows the time series of the first SVD mode, which explains 60.3% of the squared covariance between the two data sets, three times the squared covariance explained by the second SVD mode (17.8%). Thus, we only consider the leading SVD mode. Note that this first SVD mode is essentially the same even if respective linear trends at individual stations are removed. The two time series of the first SVD mode are well correlated ($r = 0.76$) and exhibit prominent decadal variability, which is especially true of the time series for the satellite data (hereafter TA1). The values of the two time series in the first SVD mode were generally greater than the mean in the early 2000s and 2010, and less than

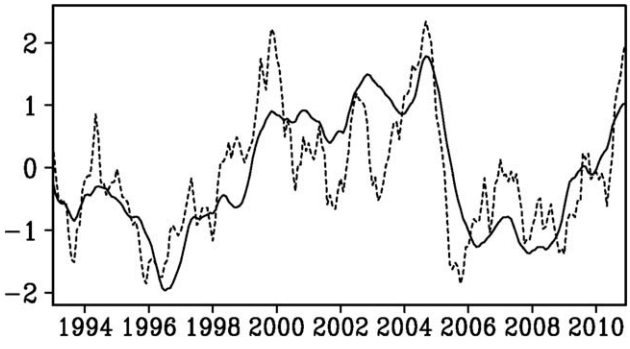

Figure 3. Normalized time series of the first SVD mode between SLAs of satellite data (solid line) and PSMSL tide-gauge data (dashed line) from January 1993 to December 2010.

the mean in the late 1990s and the late 2000s. Their period is likely different from the previously reported bidecadal fluctuations [*Senjyu et al*., 1999; *Yasuda and Sakurai*, 2006] or 18.6 year tidal cycle [e.g., *Gratiot et al*., 2008]. The time series for the tide-gauge data also exhibited interannual variability that was superimposed on the decadal variability. The linear trends of both time series were not statistically significant at the 95% confidence level, partly because the global mean sea-level trend had been removed from all sea-level time series prior to conducting the SVD analysis. Nevertheless, it is worthwhile to note that these time series show an apparent linear trend component due to the decadal nature of the increase and decrease. For example, TA1 shows a linear trend of $+3.69 \times 10^{-2}$ yr^{-1} from 1993 to 2010. This trend component contributes a sea-level rise during the satellite era and will be further discussed in section 4.

[10] We also separately used empirical orthogonal function (EOF) analysis to examine the dominant sea-level variability along the coast of Japan and in the western North Pacific. The first EOF modes of the coastal sea levels along Japan (PSMSL data) and SLAs in the western North Pacific (altimeter data) account for 43.8% and 22.1% of total sea-level variance, respectively (not shown). The corresponding principal component of the first EOF mode of coastal sea level is highly correlated with the time series for the tide-gauge data of the first SVD mode ($r = 0.98$). Similarly, the principal component of the first EOF mode of SLAs in the western North Pacific is highly correlated with the time series of the satellite of the first SVD mode ($r = 0.93$). Therefore, the first SVD mode shown in Figure 3 captures the dominant covariability between along the coast of Japan and in the western North Pacific.

[11] It is informative to note the relation of the TA1 with climate indices. We estimated the lag-correlation coefficients of TA1 with the Pacific Decadal Oscillation (PDO) [*Mantua et al*., 1997] and North Pacific Gyre Oscillation (NPGO) [*Di Lorenzo et al*., 2008] indices, which are two dominant modes in the North Pacific. The PDO index is correlated with TA1 ($r = -0.50$, significant at 95% confidence level), when TA1 lags by 36 months. The NPGO index is also correlated with TA1 ($r = 0.76$, significant at 95% confidence level), when TA1 lags by 22 months. Hence, TA1 are related to both modes. Nevertheless, it is difficult to separate the effects of the two climate modes, because the PDO index is correlated with the NPGO index during the satellite era [e.g., *Qiu and Chen*, 2010].

3.2. Coastal Sea-Level Variability

[12] The heterogeneous correlation coefficients of the coastal sea levels of the PSMSL tide-gauge data onto TA1 exhibit in-phase coastal sea-level fluctuations with strong spatial dependency (Figure 4a). Large, positive correlation coefficients are found along the southeastern coast of Honshu, which is Japan's largest island. In addition, the correlations in the western part of Japan are generally positive and statistically significant. On the other hand, the correlations along the eastern coast of Honshu north of 36°N and the entire coast of Hokkaido, the second largest island of Japan, are quite weak and statistically insignificant. Around the southeastern coast of Honshu (enlarged view in Figure 4c), which is the most densely populated area of Japan, the correlations are generally large and their spatial contrast is quite clear over the Boso Peninsula with strong and weak correlations to the west and east, respectively, of the southern tip of the peninsula. It is worth noting that the homogeneous correlation map of the coastal PSMSL tide-gauge sea-level data onto the time series for the tide-gauge data of the first SVD mode also shows a similar spatial pattern (not shown). Thus, this spatial pattern represents dominant sea-level variability of the coast of Japan. This spatial contrast will be further discussed later.

[13] Consistently, the spatial distribution of the heterogeneous regression coefficients along the coast of Japan (Figure 4b) is quite similar to that of the heterogeneous correlation coefficients (Figure 4a). The highest sea-level change is found along the southeastern coast of Honshu with an amplitude of 30 mm (Figure 4d). The SLAs in the western coast of Japan were moderate with amplitudes of 10 to 20 mm. Hence, this spatial structure indicates that sea-level rise occurred along the coast of Japan in the early 2000s and 2010, while sea-level fall occurred in the late 1990s and the late 2000s (Figures 3 and 4).

[14] As an example of the large coastal sea-level fluctuations associated with the first SVD mode, Figure 5 shows the PSMSL time series of sea-level data along the southeastern coast of Japan at the Shimizu-minato station (35.01°N, 138.52°E) and the Yaizu station (34.87°N, 138.33°E), the locations are shown in Figure 4d. The SLAs at these two stations show essentially the same temporal changes as TA1 in that sea level was high in the early 2000s and 2010 and low in the 1990s and the late 2000s, and all SLAs were highly correlated with TA1 ($r = 0.76$ and 0.87). The corresponding regression coefficients of the Shimizu-minato and Yaizu stations are 33.4 and 40.0 mm, respectively. Since the global mean sea-level rise of $+3.0$ mm yr^{-1} had already been subtracted from the tide-gauge data, long-term sea-level variability of these two stations is well explained by the sum of a globally uniform sea-level rise and the ocean circulation changes associated with the first SVD mode.

[15] The GPS corrected tide-gauge data confirm this spatial dependence (Figure 6), although the density of these tide-gauge stations is less than the distribution of PSMSL tide-gauge stations. The large SLAs are found along the southeastern coast of Japan, consistent with those of the PSMSL tide-gauge data (Figure 4). The amplitude of the regression coefficients in this region is also similar to that of the PSMSL data. Furthermore, the correlation coefficients along the eastern coast of Japan were not statistically significant and, thus, a great spatial contrast in the correlations was also found between the eastern coast and southeastern coast of Honshu. The regression and correlation coefficients of the GPS corrected SLAs onto the time series for the tide-gauge data of the first SVD mode show a great spatial contrast (not shown). Note that because the period of the GPS corrected data is shorter than that of the PSMSL data, the correlation coefficients in Figure 6a tend to be larger than those in Figure 4a. Therefore, we can conclude that the spatial dependence of SLAs along the coast of Japan determined from the PSMSL data does not result from vertical movements of the land.

[16] Great spatial differences in the correlations over the Boso Peninsula and around the southeastern coast of

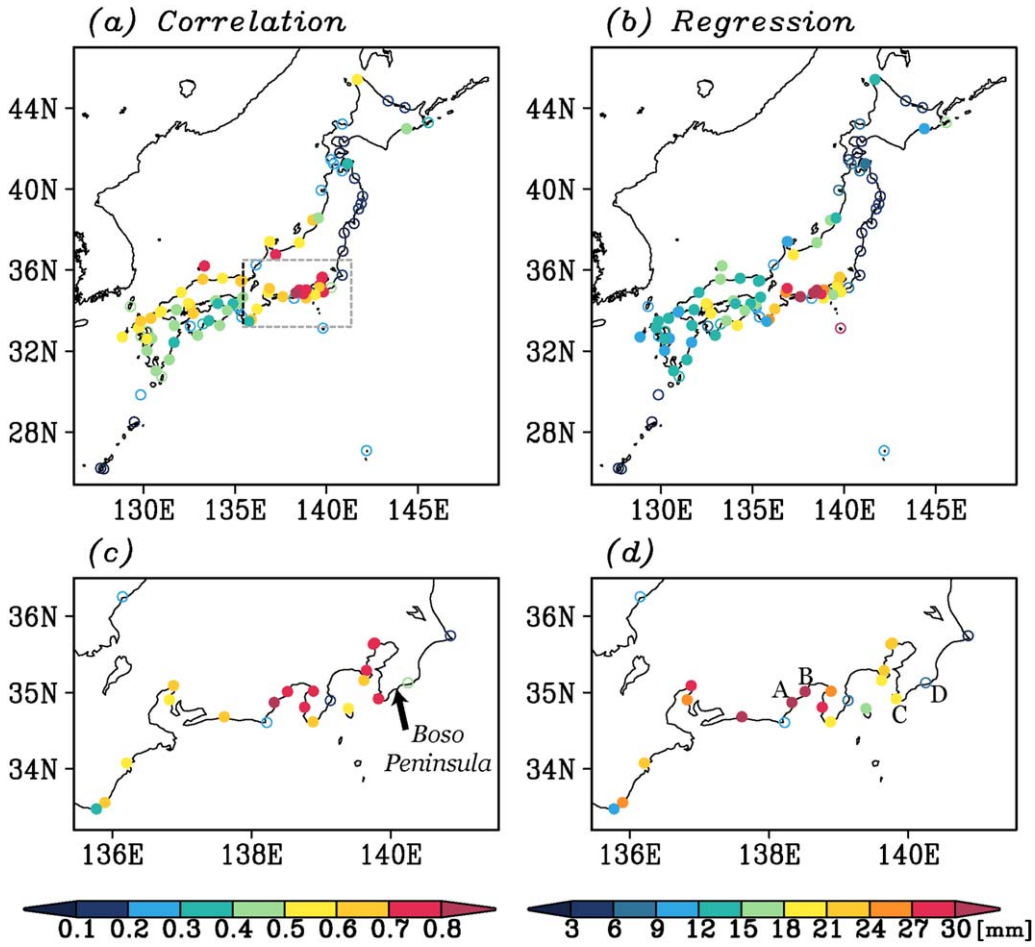

Figure 4. (a) Correlation and (b) regression coefficients of SLAs of the tide-gauge data obtained from PSMSL onto TA1. The closed and open circles denote that the correlation at that point is statistically significant or insignificant, respectively, at the 95% confidence level. (c) and (d) Enlarged views of the (a) correlation and (b) regression coefficients for the southeastern coast of Japan shown in the gray box in Figure 1a, respectively. The labels A, B, C, and D denote the Yaizu station (34.87°N, 138.33°E), the Shimizu-minato station (35.01°N, 138.52°E), Mera station (34.92°N, 139.83°E), and the Katsuura station (35.13°N, 140.25°E), respectively.

Honshu are shown in Figures 4c and 6a. A closer look at this area shows that the sea-level variability of the Mera station (34.92°N, 139.83°E) is highly correlated with TA1, but the sea-level variability at Katsuura (35.13°N, 140.25°E), which is only about 44.7 km northeast of the Mera station, is not statistically correlated with TA1 (their locations are shown in Figure 4d). Further, the sea-level variations along the southeastern coast of Honshu and west of the Mera station were well correlated with TA1, while those north of the Katsuura station were not correlated with TA1. Consistently, the correlation between the GPS corrected sea-level variability at Katsuura and TA1 is quite small ($r = 0.20$; Figure 6a). In addition to the first SVD mode, the standard deviation of sea level from the PSMSL data shows the similar large contrast along the southeastern coast of Japan (Figure 7). This result supports the great spatial differences there. Because the southeastern coast of Honshu is close to the separation point of the Kuroshio from Japan (see Figure 1), this large spatial contrast of sea-level change is expected to result from changes in the Kuroshio and the KE, which will be examined in the next subsection.

3.3. Changes in Ocean Circulation

[17] To understand the relation between the decadal sea-level variability along the coast of Japan and large-scale ocean circulation changes, we calculated the regression coefficients of the satellite-derived SLAs against TA1 (Figure 8). The strong positive SLAs, which had maximum amplitudes of about 20 cm, were located along the KE jet (also see Figure 1a) and are sandwiched by weak negative SLAs to north and south. The positive SLAs also extend westward to the south of the southeastern coast of Honshu, where the Kuroshio separates from the coast of Japan. The regression map of SLAs onto the time series for the tide-gauge data of the first SVD mode exhibits a similar pattern (not shown). The fact that the large SLAs confined along the KE jet axis suggests its meridional shift. In addition, the positive SLAs located to the south of the southeast of Honshu are also related to the northward shift of the

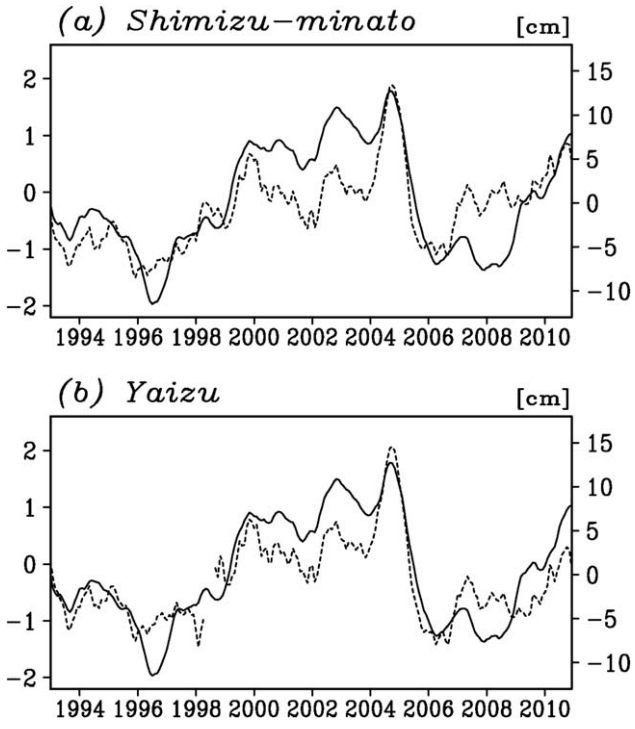

Figure 5. SLAs (dashed line; right axis) at (a) Shimizu-minato and (b) Yaizu along with TA1 (solid line; left axis). The locations of these two stations are shown in Figure 4d.

Kuroshio path there, suggesting covariation between the Kuroshio path and the KE jet path [e.g., *Sugimoto and Hanawa*, 2012]. This sea-level change is not related to the large meander path of the Kuroshio south of the coast of Japan, which causes large sea-level changes along the southern coast of Japan [*Kawabe*, 1987; *Senjyu et al*., 1999]. This more northward path of the Kuroshio around the southeastern coast of Japan appears to be consistent with the large coastal positive SLAs there (Figure 4b).

[18] TA1 is strongly related to the latitude of the KE jet averaged over 140°–165°E ($r = 0.89$; Figure 9). The latitude of the KE jet is defined by the isopleth of sea surface height that has a maximum surface velocity [for further information, see *Sasaki et al*., 2013]. Thus, the first SVD mode captures the meridional shifts of the KE jet on decadal timescales. The regression coefficient between the two time series is 0.40°. This result suggests that when the KE jet shifts northward by 1°, the sea level at Yaizu and Shimizu-minato raise by about 10.0 and 8.4 cm, respectively (see Figure 5). Note that TA1 leads the strength change of the KE jet by 5 months ($r = 0.83$; not shown). This is consistent with the results of *Sasaki et al*. [2013], who showed that the northward (southward) shift of the KE jet leads to the strengthening (weakening) of the jet. From an inspection of Figures 4d and 8, this strengthening of the KE jet is likely accompanied by the strengthening of the Kuroshio near the southeastern coast of Japan. This strengthening of the Kuroshio may act to reduce the positive SLAs along the southeastern coast of Japan, because the strengthening of the Kuroshio is generally related to negative coastal SLAs [e.g., *Imawaki et al*., 2001].

[19] What mechanism is responsible for the meridional shifts of the KE jet? Decadal variability in the KE region is primarily attributed to westward propagating signals from the central and eastern North Pacific [e.g., *Schneider and Miller*, 2001; *Qiu*, 2003; *Kwon and Deser*, 2007; *Taguchi et al*., 2007; *Sasaki and Schneider*, 2011a]. To investigate westward propagating signals, we calculated lead-lag regression coefficients of SLAs in the North Pacific onto TA1 (Figure 10). As previously reported and showed a similar figure [*Sasaki et al*., 2013, Figure 6], the positive SLAs emerged in the eastern North Pacific 3 years before the shift of the KE jet (Figure 10b), and this signal propagated westward (Figures 10c–10e). Although this westward propagation appears to resemble the traditional long Rossby wave feature [e.g., *Wu and Liu*, 2002; *Yasuda and Sakurai*, 2006], whose importance has been suggested by previous studies

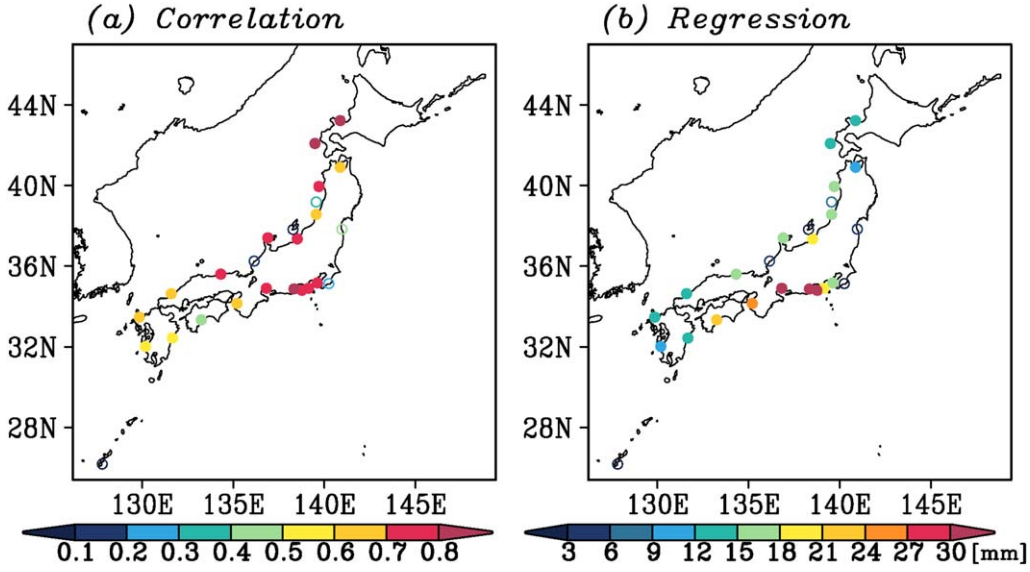

Figure 6. Same as Figure 4, but for the tide-gauge sea-level data obtained from the Geodetic Observation Center in the Geospatial Information Authority of Japan.

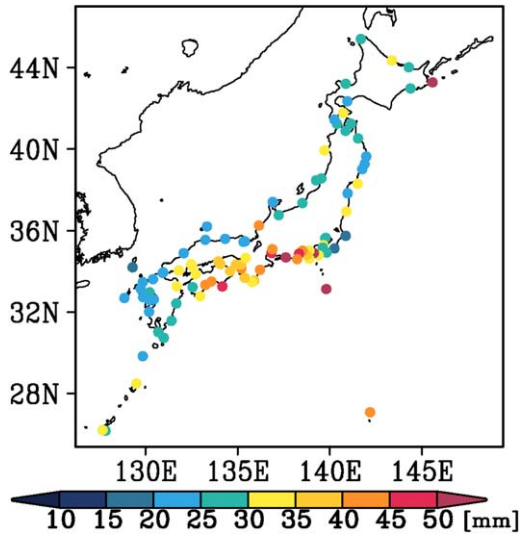

Figure 7. Standard deviation of sea level of the tide-gauge data obtained from PSMSL.

[e.g., *Cui et al*., 1995; *Yasuda and Sakurai*, 2006], traditional long Rossby waves cannot explain the westward amplitude increase accompanied by meridional scale decrease with the signal concentrating on the jet axis during the propagation. *Sasaki et al*. [2013] reported that this concentration of the SLAs on the KE jet can be explained by the jet-trapped Rossby waves [*Sasaki and Schneider*, 2011a] and results from the interaction of the waves with the KE jet. The jet-trapped Rossby wave propagates westward along the jet axis as meridional shifts of the jet, and induces meridional shifts of the upstream jet [*Sasaki and Schneider*, 2011a; *Sasaki et al*., 2013]. Therefore, the jet-trapped Rossby wave propagating from the eastern North Pacific yields the decadal sea-level variability along the coast of Japan.

[20] This incoming Rossby wave is consistent with the positive SLAs along the coast of the western Japan (Figure 4). Response of coastal sea levels to incoming Rossby waves has been investigated by many studies [e.g., *Liu et al*., 1999; *Firing et al*., 1999; *Wu and Liu*, 2002; *Tsujino et al*., 2008]. After reaching the eastern coast of Japan, the incoming Rossby wave is expected to propagate southwestward along the coast of Japan as Kelvin and coastal trapped waves, part of which reach to the western part of Japan [*Wu and Liu*, 2002; *Tsujino et al*., 2008]. This mechanism is consistent with the coastal sea-level changes observed along the western coast of Japan (Figure 4). It is worth noting that the presence of the KE jet produces an "active zone" and a "shadow zone" in terms of coastal sea-level variability (Figure 11). Initially, the SLAs in the eastern North Pacific have a large meridional scale (Figure 10b). If there was no KE jet, an incoming Rossby wave would keep a large meridional structure, and would hit the eastern coast of Japan [*Wu and Liu*, 2002]. Under this mechanism, the Rossby wave would affect sea-level variability along the entire eastern coast of Honshu, and the resultant sea-level change would be higher in the southern part of Japan due to the cumulative effect of the incoming Rossby waves [*Tsujino et al*., 2008]. However, the initial large-scale SLAs in the eastern North Pacific concentrate onto the KE jet axis in the course of propagation as a jet-trapped Rossby wave (Figure 10), and do not enter the north of the KE region [*Sasaki et al*., 2013]. Furthermore, even if a part of SLAs in the eastern North Pacific is not trapped by the KE jet, the linear long Rossby waves do not propagate into the north of the KE region [e.g., *Qiu*, 2003]. Hence, there is only small influence of incoming Rossby waves on the eastern coast of Honshu. Because the amplitude of coastal waves is determined by incoming Rossby waves from the east [e.g., *Liu et al*., 1999; *Wu and Liu*, 2002; *Tsujino et al*., 2008], and because coastal waves propagate with the coast to its right in the northern hemisphere, the eastern coast of Honshu becomes the shadow zone. Furthermore, since the Kuroshio path around the separation point from the coast of Japan also shifts northward associated with the northward shift of the KE jet (Figure 8), the coastal sea-level change is the largest along the southeastern coast of Honshu (active zone in Figure 11).

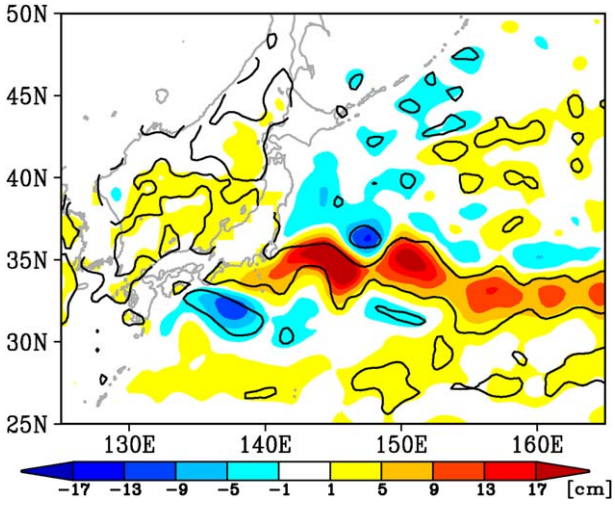

Figure 8. Regression coefficients of SLAs of the satellite data onto TA1. The contour indicates the regions where the corresponding correlations are significant at the 95% confidence level.

4. Summary and Discussion

[21] Decadal sea-level variability along the coast of Japan and its relation to large-scale ocean circulation changes from 1993 to 2010 were investigated by

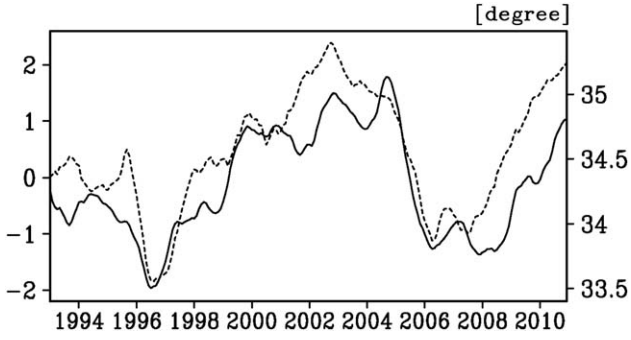

Figure 9. TA1 (solid line; left axis) and the latitude (dashed line; right axis) of the KE jet averaged over 140° to 165°E.

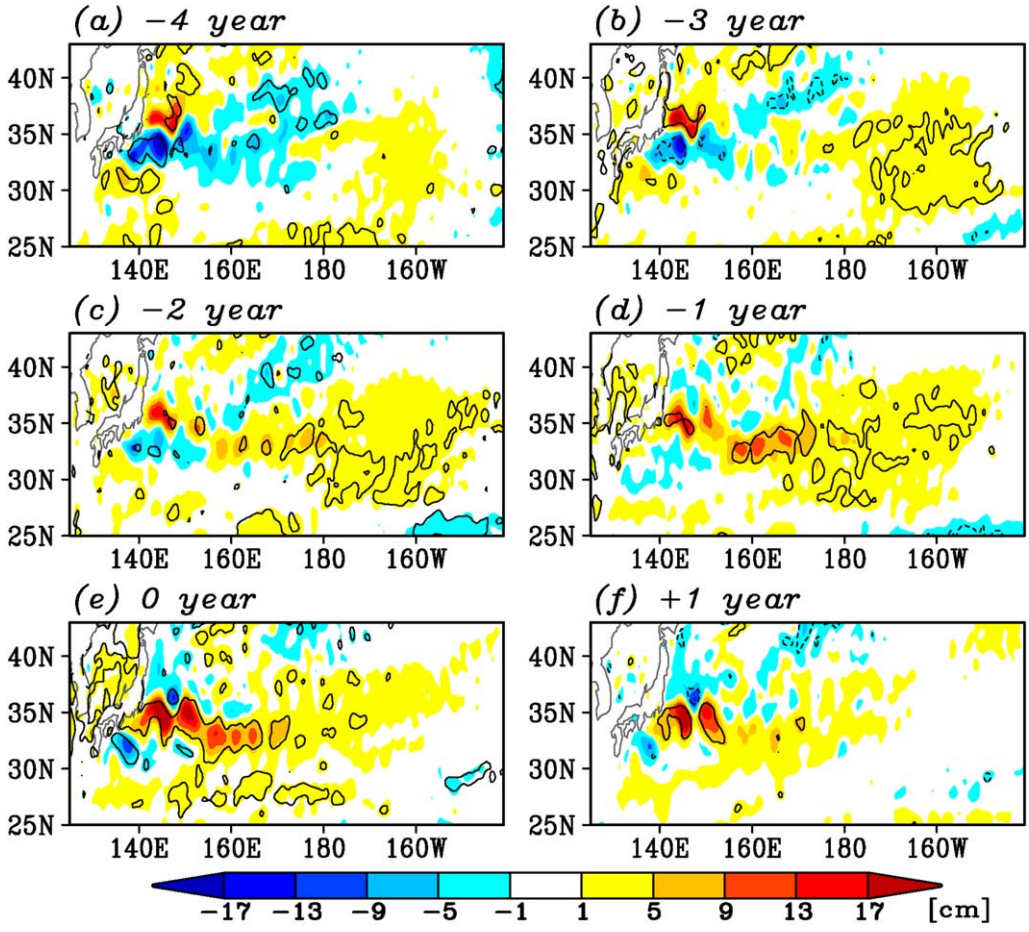

Figure 10. Lag regressions of SLAs of the satellite data onto TA1 for the number of lag years: (a) −4, (b) −3, (c) −2, (d) −1, (e) 0, and (f) +1. A negative number indicates that TA1 lags the satellite data SLAs. The contour indicates correlations that are significant at the 95% confidence level.

conducting SVD analysis on two tide-gauge data sets (Figure 1) and a satellite altimeter data set. The first SVD mode between the coastal sea levels of Japan and SLAs in the western North Pacific exhibited prominent decadal variability, which shows a coastal sea-level rise in the early 2000s and 2010 and a coastal sea-level fall in the late 1990s and the late 2000s (Figure 3). These coastal sea-level variations are not spatially uniform, but have a large spatial contrast (Figure 4). The sea-level changes were at a maximum along the southeastern coast of Honshu and were also large along the western coast of Japan (Figures 4 and 5). On the contrary, the sea-level change along the eastern coast of Honshu and the coast of Hokkaido was quite small. A similar spatial pattern of the coastal sea-level change was obtained from the GPS corrected tide-gauge data (Figure 6) and the standard deviation of sea level from the PSMSL data (Figure 7). Thus, this strong spatial dependency of the coastal sea-level change of Japan does not result from vertical land movement and is attributed to large-scale ocean circulation changes.

[22] The large-scale ocean circulation changes corresponding to these coastal sea-level fluctuations are confined along the KE jet and the Kuroshio southeast of Japan (Figure 8), indicating meridional shifts of these western boundary currents on decadal timescales (Figure 9). This decadal displacement of the KE jet is induced by jet-trapped Rossby waves propagating from the eastern North Pacific (Figure 10), as previously reported by *Sasaki et al*.

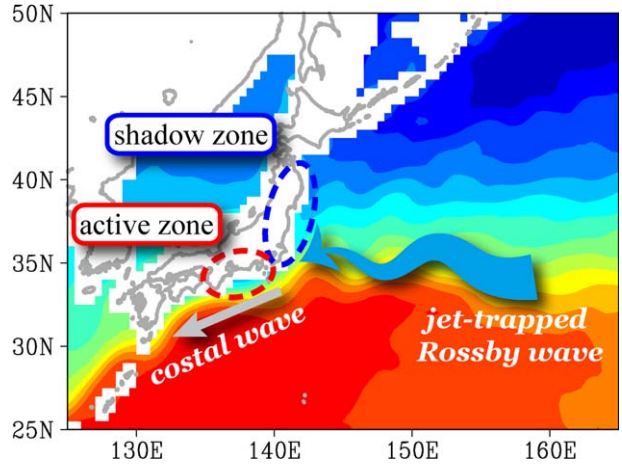

Figure 11. Schematic diagram illustrating the mechanism of the sea-level changes along the coast of Japan. The blue arrow denotes the incoming jet-trapped Rossby wave, and the gray arrow denotes coastal waves in response to the incoming jet-trapped Rossby wave.

[2013]. Since the waves propagate southwestward along the coast of Japan as Kelvin and coastal trapped waves after reaching the western boundary [e.g., *Wu and Liu*, 2002; *Tsujino et al*., 2008], the sea-level change along the North Pacific coast of Japan is large and quite small south and north of the KE jet latitude, respectively. Hence, the nature of the wave trapped by the KE jet results in the large sea-level change along the southeastern coast of Honshu (Figures 4c and 4d), which is the most densely populated area of Japan (Figure 11). Since the linear sea-level rise of 3.0 mm yr^{-1} is subtracted before the analysis (Figure 2), sea-level change along the coast of Japan from 1993 to 2010 is understood as the sum of the uniform sea-level rise of 3.0 mm yr^{-1} and the decadal sea-level variability caused by the incoming jet-trapped Rossby waves from the east.

[23] The decadal sea-level fluctuations captured by the first SVD mode contribute to the sea-level rise in the western North Pacific during the satellite observation period. The decadal variations of TA1 have an apparent linear trend of $+3.69 \times 10^{-2}$ yr^{-1} during the period from 1993 to 2010 (Figure 3), as mentioned in section 3.1. Since the corresponding regression coefficients of SLAs are about 20 cm in the KE region (Figure 8), the first SVD mode induces an apparent sea-level trend with amplitude of about +7.38 mm yr^{-1} in the KE region, which is twice the global mean sea-level rise in the same period.

[24] The findings of this study have implications for future coastal sea-level changes. As mentioned in the introduction, climate modeling studies suggest that the sea level in the subtropical North Pacific is projected to rise substantially under a global warming scenario [e.g., *Meehl et al*., 2007; *Yin et al*., 2010]. Consistently, the results of the multimodel ensemble mean of the Coupled Model Intercomparison Project phase 3 (CMIP3) model suggest that the KE jet will shift about 0.6° north in the 2060s–2090s compared to the position observed in the 1960s–1990s [*Sueyoshi and Yasuda*, 2012]. If this is the case, the sea level around the southeastern coast of Japan may rise as much as 7.0 cm (see Figure 4c), because when the KE jet shifts northward by 1°, the sea-level rise at Yaizu is by about 10.0 cm, as mentioned in section 3.3. This sea-level rise might superimpose globally uniform sea level rise (e.g., about 30.0 cm; if the trend in sea-level rise is assumed to be the same as that from 1993 to 2010) and decadal sea-level fluctuations, e.g., the first SVD mode shown in Figure 3. However, the future response of the KE jet to these sea-level changes has a large uncertainty. There is a large spread of the KE jet shift across models from about 2.2° to about −0.5° [*Sueyoshi and Yasuda*, 2012]. It is also uncertain whether the KE jet accelerates [e.g., *Sakamoto et al*., 2005] or shifts northward [e.g., *Sato et al*., 2006] for twenty-first century climate projections mainly due to the difference of atmospheric response to the global warming [*Sueyoshi and Yasuda*, 2012]. The response of the sea level depends on not only models but also the spatial resolution of the ocean general circulation model [*Suzuki et al*., 2005]. Our results indicate that the correct representation of western boundary currents in an ocean model is necessary for the reliable prediction of the future coastal sea-level changes. Reasonable choices for this purpose are downscaling using a regional ocean model that includes the entire western boundary current (e.g., west of 180° in the KE jet).

[25] **Acknowledgments.** We thank the editor and three anonymous reviewers for comments that helped to improve the manuscript. This research was supported by the Grant-in-Aid for Scientific Research on Innovative Areas grant 22106008 and for Young Scientists (B) grant 25800258, which are all funded by the Ministry of Education, Culture, Sports, Science, and Technology of Japan.

References

Anderson, D. L. T., and P. D. Killworth (1979), Non-linear propagation of long Rossby waves, *Deep Sea Res., Part A*, *26*, 1033–1050.

Bindoff, N. L., et al. (2007), Observations: Oceanic climate change and sea level, in *Climate Change 2007: The Physical Science Basis. Contribution of Working Group I to the Fourth Assessment Report of the Intergovernmental Panel on Climate Change*, edited by S. Solomon et al., Cambridge Univ. Press, Cambridge, U. K.

Bretherton, C. S., C. Smith, and J. M. Wallace (1992), An intercomparison of methods for finding coupled patterns in climate data, *J. Clim.*, *5*, 541–560.

Bromirski, P. D., A. J. Miller, R. E. Flick, and G. Auad (2011), Dynamical suppression of sea level rise along the Pacific coast of North America: Indications for imminent acceleration, *J. Geophys. Res.*, *116*, C07005, doi:10.1029/2010JC006759.

Cazenave, A., and R. S. Nerem (2004), Present-day sea level change: Observations and causes, *Rev. Geophys.*, *42*, RG3001, doi:10.1029/2003RG000139.

Church, J. A. (2001), How fast are sea levels rising?, *Science*, *294*, 802–803.

Church, J. A., J. M. Gregory, N. J. White, S. M. Platten, and J. X. Mitrovica (2011), Understanding and projecting sea level change, *Oceanography*, *24*, 130–143.

Cui, M. C., H. Vonstorch, and E. Zorita (1995), Coastal sea-level and the large-scale climate state: A downscaling exercise for the Japanese island, *Tellus, Ser. A*, *47*, 132–144.

Czaja, A., and C. Frankignoul (2002), Observed impact of atlantic SST anomalies on the North Atlantic oscillation, *J. Clim.*, *15*, 606–623.

Dee, D. P., et al. (2011), The ERA-Interim reanalysis: Configuration and performance of the data assimilation system, *Q. J. R. Meteorol. Soc.*, *137*, 553–597.

Di Lorenzo, E., et al. (2008), North Pacific Gyre Oscillation links ocean climate and ecosystem change, *Geophys. Res. Lett.*, *35*, L08607, doi:10.1029/2007GL032838.

Ducet, N., and P.-Y. Le Traon (2001), A comparison of surface eddy kinetic energy and Reynolds stresses in the Gulf Stream and the Kuroshio current systems from merged TOPEX/Poseidon and ERS-1/2 altimetric data, *J. Geophys. Res.*, *106*, 16,603–16,622.

Firing, E., B. Qiu, and W. Miao (1999), Time-dependent island rule and its application to the time-varying North Hawaiian Ridge current, *J. Phys. Oceanogr.*, *29*, 2671–2688.

Gill, A. E. (1982), *Atmosphere-Ocean Dynamics*, 662 pp., Academic, London.

Gratiot, N., E. J. Anthony, A. Gardel, C. Gaucherel, C. Proisy, and J. T. Wells (2008), Significant contribution of the 18.6 year tidal cycle to regional coastal changes, *Nat. Geosci.*, *1*, 169–172.

Holbrook, N. J., I. D. Goodwin, S. McGregor, E. Molina, and S. B. Power (2011), ENSO to multi-decadal time scale changes in East Australian Current transports and Fort Denison sea level: Oceanic Rossby waves as the connecting mechanism, *Deep Sea Res., Part II*, *58*, 547–558.

Hong, B. G., W. Sturges, and A. J. Clarke (2000), Sea level on the U.S. coast: Decadal variability caused by open ocean wind-curl forcing, *J. Phys. Oceanogr.*, *30*, 2088–2098.

Imawaki, S., H. Uchida, H. Ichikawa, M. Fukasawa, S. Umatani, and the ASUKA Groups (2001), Satellite altimeter monitoring the Kuroshio transport south of Japan, *Geophys. Res. Lett.*, *28*, 17–20.

Ishii, M., M. Kimoto, K. Sakamoto, and S. I. Iwasaki (2006), Steric sea level changes estimated from historical ocean subsurface temperature and salinity analyses, *J. Oceanogr.*, *62*, 155–170.

Kaplan, D., and L. Glass (1995), *Understanding Nonlinear Dynamics*, 420 pp., Springer, New York.

Kawabe, M. (1987), Spectral properties of sea level and time scales of Kuroshio path variations, *J. Oceanogr. Soc. Jpn.*, *43*, 111–123.

Kawabe, M. (1995), Variations of current path, velocity, and volume transport of the Kuroshio in relation with the large meander, *J. Phys. Oceanogr.*, *25*, 3103–3117.

Kwon, Y.-O., and C. Deser (2007), North Pacific decadal variability in the community climate system model version 2, *J. Clim.*, *20*, 2416–2433.

Liu, Z., L. Wu, and H. Hurlburt (1999), Rossby Wave–Coastal Kelvin Wave interaction in the extratropics: Part II: Formation of island circulation, *J. Phys. Oceanogr.*, *29*, 2405–2418.

Mantua, N. J., S. R. Hare, Y. Zhang, J. M. Wallace, and R. C. Francis (1997), A Pacific interdecadal climate oscillation with impacts on salmon production, *Bull. Am. Meteorol. Soc.*, *78*, 1069–1079.

Maximenko, N., P. Niiler, M. H. Rio, O. Melnichenko, L. Centurioni, D. Chambers, V. Zlotnicki, and B. Galperin (2009), Mean dynamic topography of the ocean derived from satellite and drifting buoy data using three different techniques, *J. Atmos. Oceanic Technol.*, *26*, 1910–1919.

Meehl, G. A., et al. (2007), Global climate projections, in *Climate Change 2007: The Physical Science Basis. Contribution of Working Group I to the Fourth Assessment Report of the Intergovernmental Panel on Climate Change*, edited by S. Solomon et al., Cambridge Univ. Press, Cambridge, U.K.

Merrifield, M. A., S. T. Merrifield, and G. T. Mitchum (2009), An anomalous recent acceleration of global sea level rise, *J. Clim.*, *22*, 5772–5781.

Minobe, S. (1999), Resonance in bidecadal and pentadecadal climate oscillations over the North Pacific: Role in climatic regime shifts, *Geophys. Res. Lett.*, *26*, 855–858.

Minobe, S. (2000), Spatio-temporal structure of the pentadecadal variability over the North Pacific, *Prog. Oceanogr.*, *47*, 381–408.

Minobe, S., T. Manabe, and A. Shouji (2002), Maximal wavelet filter and its application to bidecadal oscillation over the northern hemisphere through the twentieth century, *J. Clim.*, *15*, 1064–1075.

Miura, Y., and S. Kawamoto (2012), Analysis of sea level change with continuous GPS stations at tide gauges [in Japanese], *Kokudochiriin Jiho*, *123*, 21–33.

Nerem, R. S., D. P. Chambers, C. Choe, and G. T. Mitchum (2010), Estimating mean sea level change from the TOPEX and Jason altimeter missions, *Mar. Geodyn.*, *33*, 435–446.

Nicholls, R. J., and A. Cazenave (2010), Sea-level rise and its impact on coastal zones, *Science*, *328*, 1517–1520.

Nicholls, R. J., S. Hanson, C. Herweijer, N. Patmore, S. Hallegatte, J. Corfee-Morlot, J. Chateau, and R. Muir-Wood (2008), Ranking port cities with high exposure and vulnerability to climate extremes-exposure estimates, Environ. *Working Pap. 1*, 62 pp., Organ. for Econ. Coop. and Dev., Paris.

Onogi, K., et al. (2007), The JRA-25 reanalysis, *J. Meteorol. Soc. Jpn.*, *85*, 369–432.

Qiu, B. (2003), Kuroshio extension variability and forcing of the pacific decadal oscillations: Responses and potential feedback, *J. Phys. Oceanogr.*, *33*, 2465–2482.

Qiu, B., and S. Chen (2006), Decadal variability in the large-scale sea surface height field of the south Pacific Ocean: Observations and causes, *J. Phys. Oceanogr.*, *36*, 1751–1762.

Qiu, B., and S. Chen (2010), Eddy-mean flow interaction in the decadally modulating Kuroshio Extension system, *Deep Sea Res., Part II*, *57*, 1098–1110.

Rio, M.-H., and F. Hernandez (2004), A mean dynamic topography computed over the world ocean from altimetry, in situ measurements, and a geoid model, *J. Geophys. Res.*, *109*, C12032, doi:10.1029/2003JC002226.

Sakamoto, T. T., H. Hasumi, M. Ishii, S. Emori, T. Suzuki, T. Nishimura, and A. Sumi (2005), Responses of the Kuroshio and the Kuroshio extension to global warming in a high-resolution climate model, *Geophys. Res. Lett.*, *32*, L14617, doi:10.1029/2005GL023384.

Sallenger, A. H., K. S. Doran, and P. A. Howd (2012), Hotspot of accelerated sea-level rise on the Atlantic coast of North America, *Nat. Clim. Change*, *2*, 884–888.

Sasaki, Y. N., and N. Schneider (2011a), Decadal shifts of the Kuroshio Extension jet: Application of thin-jet theory, *J. Phys. Oceanogr.*, *41*, 979–993.

Sasaki, Y. N., and N. Schneider (2011b), Interannual to decadal Gulf Stream variability in an eddy-resolving ocean model, *Ocean Modell.*, *39*, 209–219.

Sasaki, Y. N., S. Minobe, N. Schneider, T. Kagimoto, M. Nonaka, and H. Sasaki (2008), Decadal sea level variability in the South Pacific in a global eddy-resolving ocean model hindcast, *J. Phys. Oceanogr.*, *38*, 1731–1747.

Sasaki, Y. N., S. Minobe, and N. Schneider (2013), Decadal response of the Kuroshio extension jet to Rossby waves: Observation and thin-jet theory, *J. Phys. Oceanogr.*, *43*, 442–456.

Sato, Y., S. Yukimoto, H. Tsujino, H. Ishizaki, and A. Noda (2006), Response of North Pacific ocean circulation in a Kuroshio-resolving ocean model to an Arctic Oscillation (AO)-like change in Northern Hemisphere atmospheric circulation due to greenhouse-gas forcing, *J. Meteorol. Soc. Jpn.*, *84*, 295–309.

Schneider, N., and A. J. Miller (2001), Predicting western North Pacific ocean climate, *J. Clim.*, *14*, 3997–4002.

Senjyu, T. (2006), Spatiotemporal variability of interdecadal sea level oscillations in the North Pacific, *J. Geophys. Res.*, *111*, C07022, doi: 10.1029/2005JC003053.

Senjyu, T., M. Matsuyama, and N. Matsubara (1999), Interannual and decadal sea-level variations along the Japanese coast, *J. Oceanogr.*, *55*, 619–633.

Sueyoshi, M., and T. Yasuda (2012), Inter-model variability of projected sea level changes in the western North Pacific in CMIP3 coupled climate models, *J. Oceanogr.*, *68*, 533–543.

Sugimoto, S., and K. Hanawa (2012), Relationship between the path of the Kuroshio in the south of Japan and the path of the Kuroshio Extension in the east, *J. Oceanogr.*, *68*, 219–225.

Suzuki, T., and M. Ishii (2011a), Regional distribution of sea level changes resulting from enhanced greenhouse warming in the Model for Interdisciplinary Research on Climate version 3.2, *Geophys. Res. Lett.*, *38*, L02601, doi:10.1029/2010GL045693.

Suzuki, T., and M. Ishii (2011b), Long-term regional sea level changes due to variations in water mass density during the period 1981–2007, *Geophys. Res. Lett.*, *38*, L21604, doi:10.1029/2011GL049326.

Suzuki, T., H. Hasumi, T. T. Sakamoto, T. Nishimura, A. Abe-Ouchi, T. Segawa, N. Okada, A. Oka, and S. Emori (2005), Projection of future sea level and its variability in a high-resolution climate model: Ocean processes and Greenland and Antarctic ice-melt contributions, *Geophys. Res. Lett.*, *32*, L19706, doi:10.1029/2005GL023677.

Taguchi, B., S.-P. Xie, N. Schneider, M. Nonaka, H. Sasaki, and Y. Sasai (2007), Decadal variability of the Kuroshio extension: Observations and an eddy-resolving model hindcast, *J. Clim.*, *20*, 2357–2377.

Timmermann, A., S. McGregor, and F.-F. Jin (2010), Wind effects on past and future regional sea level trends in the Southern Indo-Pacific, *J. Clim.*, *23*, 4429–4437.

Tsujino, H., H. Nakano, and T. Motoi (2008), Mechanism of currents through the straits of the Japan sea: Mean state and seasonal variation, *J. Oceanogr.*, *64*, 141–161.

Vinogradov, S. V., and R. M. Ponte (2011), Low-frequency variability in coastal sea level from tide gauges and altimetry, *J. Geophys. Res.*, *116*, C07006, doi:10.1029/2011JC007034.

Woodworth, P. L., and R. Player (2003), The permanent service for mean sea level: An update to the 21st century, *J. Coastal Res.*, *19*, 287–295.

Wu, L. X., and Z. Y. Liu (2002), Dynamical control of pacific oceanic low-frequency variability on western boundary and marginal seas, *Geophys. Astrophys. Fluid Dyn.*, *96*, 201–222.

Yasuda, T., and K. Sakurai (2006), Interdecadal variability of the sea surface height around Japan, *Geophys. Res. Lett.*, *33*, L01605, doi:10.1029/2005GL024920.

Yin, J., S. M. Griffies, and R. J. Stouffer (2010), Spatial variability of sea level rise in twenty-first century projections, *J. Clim.*, *23*, 4585–4607.

Zhang, X. B., and J. A. Church (2012), Sea level trends, interannual and decadal variability in the Pacific Ocean, *Geophys. Res. Lett.*, *39*, L21701, doi:10.1029/2012GL053240.